Real-Time Illustration of Vascular Structures

Felix Ritter* MeVis, Bremen
Christian Hansen MeVis, Bremen
Volker Dicken MeVis, Bremen
Olaf Konrad MeVis, Bremen
Bernhard Preim University of Magdeburg
Heinz-Otto Peitgen MeVis, Bremen

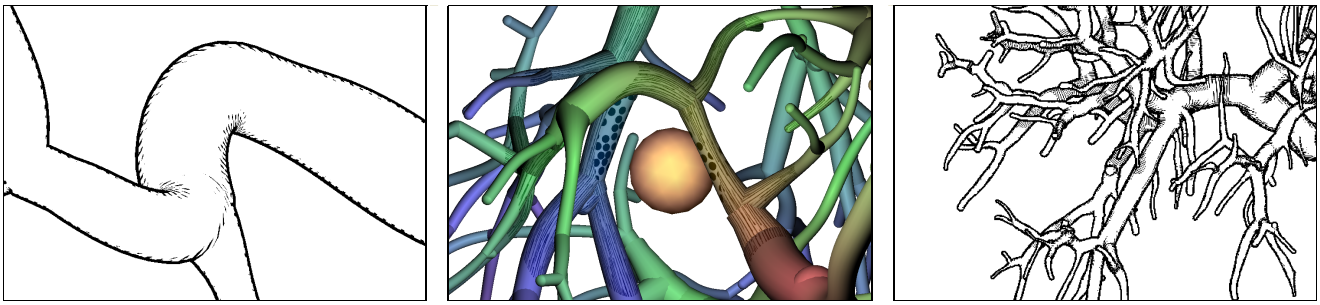

Figure 1: Examples of vascular illustrations enhancing perception of properties important in surgery. Left and right image: Hatching indicates curvature and distances; middle image: Textures indicate distances to a generalized lesion (orange)

Abstract

We present real-time vascular visualization methods, which extend on illustrative rendering techniques to particularly accentuate spatial depth and to improve the perceptive separation of important vascular properties such as branching level and supply area. The resulting visualization can and has already been used for direct projection on a patient's organ in the operation theater where the varying absorption and reflection characteristics of the surface limit the use of color. The important contributions of our work are a GPU-based hatching algorithm for complex tubular structures that emphasizes shape and depth as well as GPU-accelerated shadow-like depth indicators, which enable reliable comparisons of depth distances in a static monoscopic 3D visualization. In addition, we verify the expressiveness of our illustration methods in a large, quantitative study with 160 subjects.

CR Categories: H.1.2 [User/Machine Systems]: Software psychology, I.3.3 [Picture/Image Generation]: Display algorithms—Illustration, J.3 [Life and Medical Sciences]

Keywords: vessel visualization, functional realism, illustrative rendering, spatial perception

1 Introduction

Understanding the branching pattern and topology of vascular structures is crucial for therapy planning and the actual surgery in order to prevent healthy organs or organ regions from being cut off from blood supply and drainage. A 3D visualization that provides knowledge about the location, properties, spatial distances, and functional relationships of those vessels to other relevant anatomic structures has been a frequent request by surgeons. While current therapy planning software can provide most of this information, an integrated visualization that enables the surgeon to make reliable judgments without time-consuming, interactive inspections still remains an open request. During surgery, the surgeon has even less time to analyze complex visualizations than at the planning stage. Ideally, such visualization would therefore be static in a sense of facilitating frequent look-ups of required information yet providing all necessary morphological and spatial information in one single picture. Such a picture could be printed, displayed on a monitor inside the operation theater, and eventually projected on the very organ before dissection.

The perception of spatial distances, however, becomes demanding when viewing a static, monoscopic projection of a 3D visualization. This is especially true for complex vascular systems that may consist of multiple interweaved tree-like structures such as the vascular systems of the liver (portal vein, liver artery, hepatic veins, and biliary duct). The effectiveness and lucidity of the visualization highly depend on the accentuation of spatial depth as well as the perceptive separation of important, individual properties.

To improve the communication of both aspects, the real-time vascular visualization methods presented in this paper utilize and extend on illustrative rendering techniques that provide functional realism [8]. Illustrative visualization methods not only allow us to emphasize or omit properties, but also offer visualization techniques with limited use of color. Due to varying absorption and reflection characteristics on organ surfaces, the perceived color and brightness gradations resulting from a traditional shaded projection on the organ are difficult to predict, thus making them less suited for this purpose. Instead we propose the use of texture as an alternative visual attribute. This allows us to encode additional information, such as the local distance to a tumor.

We present new methods to convey the shape and topology of vascular structures with a new GPU-based hatching algorithm, introduce GPU-based distance-encoded surfaces and shadows improving the reliable comparison of spatial distances in a static 3D visualization and finally verify our methods in a quantitative study with 160 subjects (38 being physicians or medical students).

* e-mail: ritter@mevis.de, MeVis – Center for Medical Diagnostic Systems and Visualization, Bremen, Germany

First, we review related work in the field of vascular visualization, briefly repeat the major steps to construct a vascular model from image data and describe our approach to the generation of texture coordinates. Subsequently, we introduce new illustration techniques to enhance spatial perception and discuss our evaluation of these techniques. We conclude the paper with a summary.

2 Related Work

2.1 Visualization of Vascular Structures

For the diagnosis of vascular diseases, 2D as well as conventional 3D visualization techniques, such as direct volume rendering, maximum intensity projection and isosurface rendering, are employed. With these methods, the underlying image data are faithfully represented [23]. However, artifacts due to inhomogeneity of contrast agent distribution and aliasing problems due to the limited spatial resolution may hamper the interpretation of spatial relations. Therefore, explicit surface reconstructions of vascular structures are often preferred for surgical therapy planning and intraoperative visualization, where the interpretation of vascular connectivity and topology is more important than the visualization of vascular diseases [4].

A variety of reconstruction methods have been developed which use the skeleton of a vascular tree and the local radius information as input. Assuming a circular cross section, surfaces of vascular trees are either explicitly constructed or implicitly created by means of an implicit description. Among the explicit methods, graphics primitives such as cylinders [16] and truncated cones [11] are employed. A general problem of these methods are discontinuities, which primarily occur at branchings.

The most advanced explicit reconstruction technique is based on subdivision surfaces [7]. An initial base mesh is constructed along the vessel centerline. The base mesh consists of quadrilateral patches and can be subdivided and refined according to the Catmull-Clark scheme.

Implicit modeling is used in general to achieve smooth and organic shapes. A special variant, convolution surfaces, can be used to represent skeletal structures [3]. With careful selection of a convolution filter, this concept allows to faithfully represent the local diameter of vascular structures [17]. A comprehensive survey of methods for vessel analysis and visualization is given in [1].

While the research mentioned above has focussed on the modeling of vascular structures to convey shape and topology, we aim at improving spatial perception, particularly depth perception, and at communicating important vascular properties by using and extending illustrative visualization techniques. None of the vascular presentation techniques described in previous work has a theoretical foundation in shape perception.

2.2 Illustration of Spatial Depth

Illustrative techniques have been widely used to increase the expressiveness of visualizations. We are primarily interested in hatching due to its great potential to express shape. The advantages of hatching along curvature directions to convey shape in comparison to conventional surface shading have been emphasized in [14,15]. Praun et al. [19] developed a real-time system for rendering hatching strokes over arbitrary surfaces along curvature direction. A sequence of mip-mapped hatch images, a *tonal art map* is constructed to convey different material properties and lighting. Zander et al. [27] describe a hatching technique guided by curvature directions and suitable for anatomic structures of arbitrary shape. However, extensive preprocessing is required to achieve interactive frame rates. The shape of elongated structures, such as muscles, has been visualized directly from segmented volume data with an appropriate parameterization of hatching lines [6].

The visualization of hidden isosurfaces by means of illustrative techniques is described in [9]. House et al. [12] investigate properties of textures well-suited for the viewing of layered surfaces. Weigle and Taylor [26] show that curvature-aligned stroke-like glyphs improve perception of inter-surface distance of nested surfaces in comparison to direct color mapping. To enhance the perception of relative depth, the illumination of a surface can be attenuated by occlusions in the local vicinity of a surface point [21].

Related to the visualization of vascular trees is the visualization of natural botanic trees. Deussen and Strothotte [5] introduced an illustrative technique for botanic trees, which also employs a skeleton and derives curvature-based hatching lines.

3 Texture-based Visualization of Vessels

To encode important properties and to convey shape and topology at the same time is difficult using color only. Applying texture as an additional attribute to certain regions of the vascular structure allows for a more distinct encoding of information. We use texture to primarily express spatial properties of vascular structures important in therapy planning and surgery:

- information on distances between vascular structures,
- relative distances of depicted vascular segments to the observer,
- shape and spatial orientation, and
- distances to other relevant anatomic structures.

We combine texture with color and illustrate the following characteristics of vascular structures using color:

- type of vascular system (e.g. arterial system, venous system),
- branching level and diameter of vascular segments, as well as
- supply and drainage areas within an organ.

The figure below depicts a vascular illustration created with the methods discussed subsequently using hatching strokes and what we call *distance-encoded shadows*. Color has been used to identify supply areas within the liver.

Figure 2: Portal vein of the liver rendered using methods discussed subsequently: Color has been applied to indicate supply areas.

3.1 From Voxels to Vascular 3D-Models

We employ the method presented in [11] as a basis for the visualization of vascular structures. We briefly repeat the major steps of this method here:

1. *Segmentation* of vascular structures in the CT / MR volume data
2. *Skeletonization* with a topology-preserving thinning algorithm yielding an exact centerline and the radius at each voxel of the skeleton
3. *Graph analysis* transforming the skeleton in a directed, acyclic graph where nodes represent branchings. Each edge keeps a list of the skeleton voxels and vessel diameters
4. *Skeleton enhancement* employing pruning and smoothing
5. *Visualization* by reconstructing a 3D model

The reconstructed vascular 3D model is an assembly of truncated cones, each representing a section between two skeleton voxels. The top and bottom parts of those truncated cones are built using a discrete, circular approximation. For each skeleton voxel, the circular approximation is rotated to lie in a plane defined by the bisector of vectors to the preceding and succeeding skeleton voxel and is scaled according to the radius at the concerning skeleton voxel. Surface polygons are generated by connecting corresponding points of succeeding circular approximations. Hence, all truncated cones representing one edge consist of the same number of faces. The exact number depends on the average diameter of the segment and on a user-defined quality parameter. At the root node and the leaf nodes, a hemispherical geometry, called *leaf cap*, is generated by using a cosine function. At branchings, intermediate nodes are generated by connecting corresponding points of the stubs of each child edge to points of its parent edge.

3.2 Generation of Texture-Coordinates

Mapping a texture to a polygonal model requires parameterizing the surface by assigning texture coordinates to each vertex of the model. The generation of texture coordinates is trivial for non-complex models by using standard texture mapping approaches. For complex vascular structures, those techniques are not suitable to achieve appropriate results, since a distortion of the texture mapped images cannot be handled.

We developed a two-part texture mapping technique [2] for vascular structures that uses cylinders as intermediate geometric primitives. Utilizing topological information available from the graph analysis, we apply a separate texture mapping for each element of the graph (nodes and segments). This allows for an easy adoption of the texture mapping technique on the underlying geometric primitives (assembly of truncated cones). To prevent visible seams between successive textured primitives, the graph is traversed hierarchically, starting at the root node. Consequently, the texture coordinates of a segment are based on the texture coordinates of the preceding element.

While the two-part cylinder mapping is applied to tubular structures (like the geometry of the segments and the intermediate nodes), a sphere mapping is used to produce texture coordinates for hemispherical elements, e.g. the leaf caps. If the curvature along the skeleton line is greater than a given threshold, a recursive subdivision is applied on the affected elements in order to minimize texture distortions.

4 Enhancing Spatial Perception

4.1 Communicating Shape Using Hatching Strokes

Lighting and shading are crucial sources of information about the shape and topology of three-dimensional objects [20]. Based on traditional illustration techniques such as stippling and hatching, a variety of methods have been proposed to simulate these effects in non-photorealistic renderings. While stippling is commonly used in archeological illustrations, hatching seems more appropriate for illustrations in medicine. Hatching strokes may approximate natural light interaction and emphasize characteristic features of the surface, such as curvature and discontinuities. However, none of the drawing algorithms has been designed for the specific demands of vascular illustration and reliable perception of depth distances.

Since we represent the vascular branches by a more or less smooth surface assembled of truncated cones, discontinuities appear almost exclusively at branchings. Larger discontinuities within a branch, such as aneurysms, however, are also accentuated by the hatching algorithm proposed below. Changes in the direction of vascular segments are clearly visible and require no special emphasis if the tangent vector of the centerline is nearly perpendicular to the line of sight. In these cases, the silhouette indicates the curvature sufficiently. Things become different, however, in direction of the line of sight. Changes in the direction toward or against the observer must be accentuated to be perceived (see Figure 3).

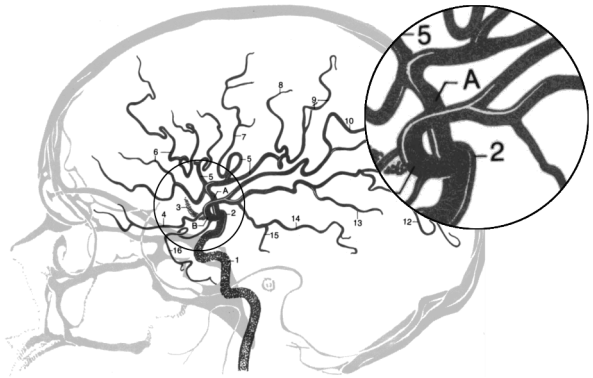

Figure 3: This book illustration has inspired our work. The curvature of the vessels is indicated only at a few necessary locations.

The new image-based hatching algorithm uses depth differences computed from discretized depth values of two renditions different in size to determine not only a location where strokes should be drawn but to produce the silhouette and strokes themselves. To obtain the first depth image, the unchanged vascular model is rendered with a fragment (pixel) shader that limits the total number of different depth values (N). Thus, the fragments' values are clustered generating a depth image, in which distance-dependent, discontinuous steps replace otherwise continuous gradients.

$$d_{\text{stored}} = \text{floor}(d_{\text{fragment}} \cdot N)/N \quad (1)$$

A second rendition of the model uses a vertex shader in addition to the fragment shader to relocate all vertices in direction of their normal vector by a small, fixed value (T) thus slightly enlarging the model. The depth buffer of the first rendition is read by the fragment shader to compute the unsigned difference of the current

fragment's discretized depth value to the also discretized depth value of the first rendition. The computed value is stored in a special depth-difference buffer. Also, the unchanged depth value is stored in the regular depth buffer for later use. Figure 4 depicts the resulting image stored in the depth-difference buffer using a simple cylinder.

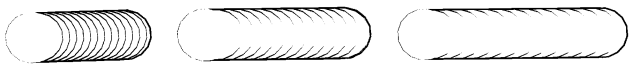

Figure 4: Contrast enhanced depth difference image: The orientation of the cylinder changes from left to right toward the user, demonstrating the disappearance of strokes that indicate depth along the cylindrical surface. *N*=256

The image created by the algorithm described above already produces a silhouette and strokes that enhance the depth perception of the surface. Strokes are only drawn at surface locations almost perpendicular to the line of sight. To increase or decrease the amount of strokes, the discretization of depth values (*N*) may be modified. A modification of the vertex relocation value (*T*) directly influences the silhouette and stroke width.

In order to increase the impression of irregularity in the placement of strokes, we combine the depth-difference image with a third rendition of the model that uses a fixed procedural stroke texture (Figure 5).

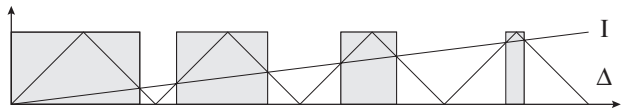

Figure 5: Procedural hatching stroke texture: Strokes are created by evaluating a triangle function Δ and a continuous function I. Texels are black if $\Delta(x) > I(x)$, otherwise white. Idea by B. Freudenberg [10].

Only fragments that form strokes are affected. Hence, no new strokes are added, but existing strokes are thinned and split. Figure 6 shows the effect of the texture's stroke frequency as it is controlled by the slope of the triangle function Δ on the final image.

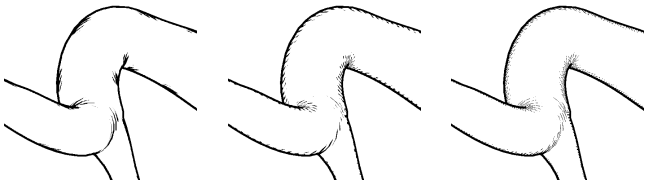

Figure 6: The effect of stroke frequency variation: The frequency increases from left to right.

4.2 Generation of Distance-Encoded Shadow

Shadow has long been recognized as a valuable cue to estimate spatial distances [21,25]. To be valuable in perceiving spatial depth in the depiction of vascular structures, small depth differences must be brought to attention in a way that enables the observer to reliably compare depth distances. At the intersection of vascular structures occlusion indicates order, however, the distance of the segments remains unknown. The sole integration of accurately simulated shadow does not improve this situation. Shadows cast onto vascular segments by structures closer to a camera-attached point light source will change in size depending on the distance. However, to be clearly distinguishable and to allow for precise depth judgments, the indication must provide more fine grain control.

Based on the visual metaphor of a shadow we incorporate hatched depth indicators that are more sensitive to small depth differences and call them *distance-encoded shadows*. As recommended by studies on the spatial perception effect of shadow quality [24] and quantity [13], we draw just a single filled outline. Size and texture of the shadow can be modified allowing a double encoding of depth (Figure 7).

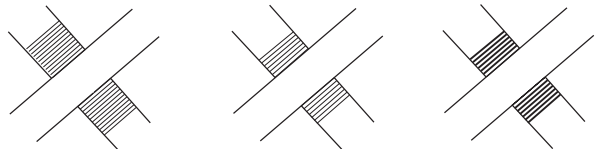

Figure 7: Visualization of depth at the intersection of vascular structures: The middle and right illustrations indicate a smaller distance than at the intersection in the left illustration. In the right illustration a double encoding is used that also darkens smaller shadows.

Before applying texture, the region to be covered must be determined. Again, depth differences are used to create a mask image containing regions of shadow. This time, however, depth values are not discretized. Figure 8 illustrates the important steps of the algorithm outlined below.

A depth difference image is obtained in a two pass rendering process by relocating all vertices in direction of their normal during the second pass and computing the difference to the first, regularly rendered depth image for each fragment. Subsequently, all pixels being classified as background in the rendition of the regular-sized model are discarded from the depth difference image. Also, pixels with a value less than or equal to the vertex relocation value *T* are discarded. In the end, pixels with a value greater than zero represent shadow. If the depth images are obtained using an orthographic projection, which is common in medical visualizations and the method of choice for an image that eventually will be projected onto an organ's surface, the pixel values can be compared directly to evaluate distance. For perspective projection, the relationship between distance and the depth buffer value is non-linear, thus requiring an extra transformation.

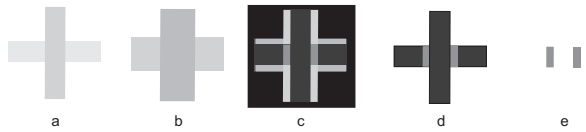

Figure 8: Determination of shadow regions: Computing a depth difference image (c) from a regular-sized (a) and an enlarged rendition's depth buffer image (b). All pixels in (c) being background in (a) are discarded (d). Using the vertex relocation value *T* as a threshold all pixels with values less than or equal to *T* are discarded too, leaving just the shadow mask (e).

Obviously, the shadow length depends on the relocation value *T*. Hence *T* should somehow be related to the distance at the intersec-

tion of two vascular segments. Beside using just a linear mapping, an exponential dependency allows for a more sensitive visualization of small variations. This becomes more crucial for the illustration of large, complex vascular systems, where the perceived size of the shadow indicators is generally smaller. Also for surgical purposes, it is often sufficient to draw distance-encoded shadows only locally, e.g. to emphasize depth only in the vicinity of a tumor.

In order to compute the depth distance D at intersections and to draw a shadow, the following approach is taken. Exploiting multiple shadow masks of different sizes and the original depth image obtained during the creation of the shadow mask image with the largest relocation value T (referred to as Z_{max}), the vascular model is rendered in regular size. For each fragment to be drawn, the corresponding value from the depth image Z_{max} is used to compute the depth distance. Using the biggest rendition of the vascular structures as the reference ensures that this difference can be computed for all fragments that are possibly part of a shadow. Depending on the distance value, one of the shadow masks is evaluated to decide whether or not the fragment is eventually drawn as shadow.

The distance D is used during the shadow drawing process to darken the perceived brightness of a procedural hatching texture representing the shadow. Smaller shadows are drawn darker than larger shadows. This corresponds to the perception of real shadows caused by a point light source. The orientation of the hatching strokes can be changed, too. An evaluation of the stroke direction (see Section 6) shows a strong preference of strokes that emphasize the principal curvature of the vascular structures.

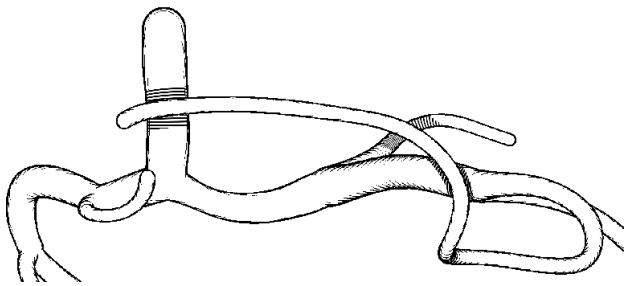

Figure 9: Indicating depth distances at intersections in a real vascular structure using distance-encoded shadows: The size of the drawn shadow at an intersection corresponds directly to the depth distance between the two overlapping vascular segments.

Obviously, the number of different shadow sizes is limited due to the dependency of the shadow mask creation process on an additional render pass. This, however, does not limit the practical application of this visualization technique for surgery. First, only a few critical vascular structures are affected by a surgical intervention. Thus, the visualization can and should focus on illustrating depth important to judge spatial relations of these vessels. Second, the discrete nature of the visualization with distance-encoded shadows does in fact facilitate the comparison of depth distances: Shadows of the same length indicate structures with approximately the same depth distance.

4.3 Encoding Observer-Relative Depth Distances

While distance-encoded shadows indicate depth between vascular segments at intersections, the distance to unoccluded vessels is difficult to judge. The observer is required to track the vascular structures along and to mentally build a 3D model from shading (hatching) information. To facilitate depth perception of those vascular segments, we developed a technique termed *distance-encoded surface*, which encodes observer-relative depth distances using hatching strokes. This technique takes advantage of depth perceived from a texture gradient. Stroke attributes are adapted using the procedural stroke texture introduced in Section 4.1.

We encode distance information by varying the width of the strokes (Figure 10). In order to calculate the required distance information, we construct a plane perpendicular to the line of sight that is located at the intersection of the vascular model's bounding sphere with the line of sight. During the rendering process, the Euclidian distance between each vertex and the plane is calculated in a vertex shader. Hence, the distance indicated by the stroke texture does not depend on the absolute distance to the observer but on the relative distance. We also calculate the angle between the surface normal at the currently processed vertex and the line of sight and use this value to prevent distortions caused by the tilt angle of the surface. Figure 10 uses a linear mapping of distance to affect the stroke width by changing the I-function illustrated in Figure 5. To enhance the expressiveness of the depth cue, again a non-linear (e.g. exponential) function may be employed.

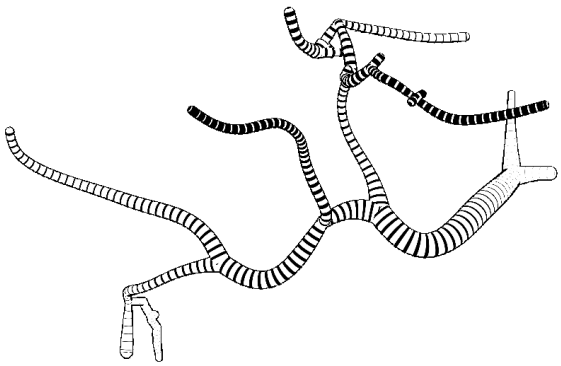

Figure 10: Encoding the distance of vascular structures to the observer by varying the stroke-width of a procedural stroke texture. Thicker black strokes indicate a shorter distance to the observer.

4.4 Distances Between Vascular Structures and a Lesion

Knowledge about the distance between major vascular branches and a lesion is important for therapy planning: Surgeons try to avoid damaging vascular structures above a certain diameter. The texture-based approaches outlined so far do not require color to communicate shape and topology, but are well suited to be combined with color. Hence, color may be used as an additional visual attribute to facilitate distinct multi-parameter visualizations (see middle image of Figure 1).

We developed discrete and continuous distance visualization techniques illustrated by the sketches in Figure 11. To achieve a discrete distance view, we map textures, which are easily distinguishable (possibly preattentively), on the vessel surface in dependence of a discrete distance function. Physicians are used to obtain distance information between vessels and lesions in discrete steps (e.g. a computed safety margin around a tumor of 1cm, 1.5cm, and 2cm). This allows clear decisions without ambiguities. As an alternative approach, a continuous distance function is used to modify the size of glyphs, as exemplified in Figure 11.

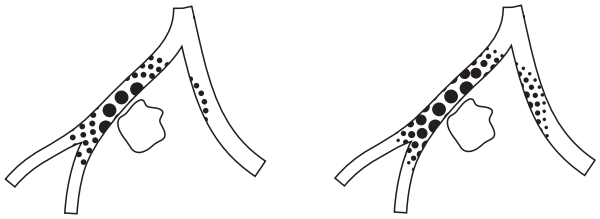

Figure 11: Sketch illustrating discrete (left) and continuous (right) distance visualization using a procedural circle texture.

5 Implementation

We implemented the previously discussed illustration techniques on top of the Open Inventor graphics library by writing nodes encapsulating OpenGL 2.0 vertex and fragment shaders and the OpenGL framebuffer object extension. A scene graph has been constructed using the research prototyping platform MeVisLab. All vertex and fragment shaders have been realized using the OpenGL shading language utilizing multiple render targets to reduce the number of render passes, e.g. writing unchanged and discretized depth values in a fragment shader simultaneously.

Using a NVidia 7800 GTX graphics accelerator, the illustration shown in Figure 13 (600×600 pixels, 67k Δ) can be rendered at 14 fps. Figure 14 (600×600 pixels, 230k Δ) renders at 8 fps. Currently, the number of polygons is the main bottleneck. However, both vascular structures are highly detailed reconstructions that show more details than are typically imaged in CT or MRI of patients.

6 Evaluation

To evaluate the effect of stroke hatching, distance-encoded surface illustration and shadow on the perception of depth in an vascular illustration, we conducted a large quantitative study. Our subject pool consisted of 77 females and 83 males (a total of 160 subjects in the age of 17 to 56 years), 38 of them being physicians or medical students. We were able to probe this large number of subjects in one week by designing a web-based questionnaire.

6.1 Experimental Design and Methodology

In order to probe the subjects' perception of depth distances, we designed tasks that require a precise judgement of depth. One task, used to evaluate the *effect of stroke hatching* and *distance-encoded surface visualization*, prompted the subjects to specify the correct order of marks on an illustration of a vascular structure, starting with the perceived shortest distance to the observer (estimated egocentric distances). Subjects had to track vascular segments along to judge and accumulate changes in surface orientation. Another task, which asked subjects to determine the order of depth distances between vascular segments at clearly marked intersections, has been employed to evaluate the *effect of distance-encoded shadow* (estimating exocentric distances). In addition to these objective measurements, we also asked subjects about their preference regarding the parametrization of some of the illustrative visualization techniques, such as the direction of hatching strokes in the distance-encoded shadows.

To be able to test a large number of subjects, we designed a web-based questionnaire using PHP and MySQL. Since we wanted to assess the effect of illustration techniques, one visualization of a vascular model using one of the new techniques had to be compared with a second visualization of the same model identical in every major aspect, except for the display algorithm. This requirement has been met by using the same model, same directional light and view. However, by presenting the same view twice and asking to judge the depth of exactly the same vascular segments, chances are high that subjects give exactly the same answer for the visualization presented secondly. Any time measurements would also be rendered invalid because of learning effects. Based on the known inability of humans to perform mental rotations [18], the view in the second visualization had been rotated about the line of sight to hamper recognition.

Given these considerations, each subject had to work on all tests. The structure of the questionnaire is shown in Figure 12, each number representing one web-page in order of appearance. Subjects could not return to a previous page and had been instructed to complete each test as fast as possible. We tested each of the visualization methods using two paired tests in different sequence. For instance, page 5 presented three marks on the surface of a vascular structure that had been visualized using hatching strokes (similar to Figure 14). The subjects had to enter the correct depth order using the numbers of the marks and press the 'next' button. Page 9 presented the pendant to page 5 using Gouraud shading to illustrate shape. The view onto the same model had been rotated around the line of sight as discussed above, the marks were at the same positions but had a different numbering. Page 6 and 10 presented the same questions with a different model in opposite sequence.

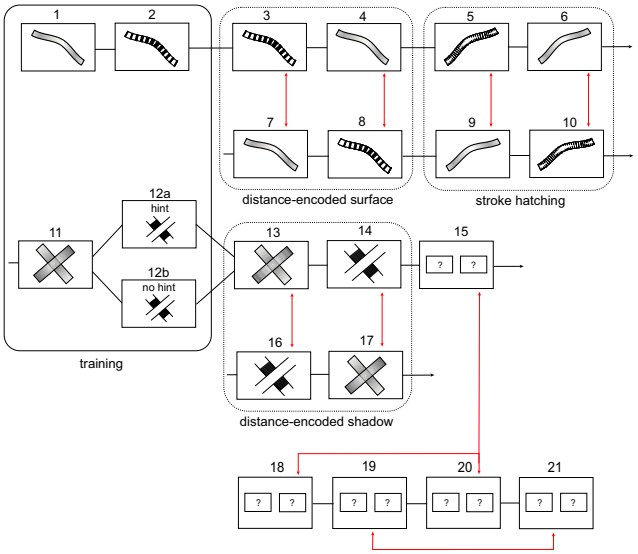

Figure 12: Diagram of the questionnaires' structure: Each number represents one page of the web-based questionnaire in order of appearance. Question marks represent subjective preference tests.

To evaluate whether or not subjects would intuitively recognize the way in which distance-encoded shadows provide depth cues, half of the subjects were given an explanation on page 12 whereas the other half did not get any hints. The last pages did ask subjects about their preferences regarding the shadow appearance: Hatching stroke direction along or diagonal to the centerline, as well as the encoding of depth by changing the length of the shadow and/or

the stroke width being candidates. Two images side by side were presented to the subjects.

6.2 Results and Discussion

We rated the results of the three main paired-tests using the following system: All three marks ordered correctly: 1; Two of three marks ordered correctly: 0.5; otherwise: 0. Given the nature of the data we had collected (dependent samples, non-parametric data) we employed the Wilcoxon signed rank test to analyze the results. To evaluate the intuitive recognition and utilization of distance-encoded shadow we used the Wilcoxon rank sum test (independent samples). In addition to the test metrics (Wilcoxon V, probability p), we report means (μ) and standard deviations (σ) for descriptive purposes in table 1.

Table 1: Statistics of the three main paired-test: *new* indicates the new approach, *trad* stands for the control condition (traditional)

	μ_{new}	σ_{new}	μ_{trad}	σ_{trad}	p	V
Surface Test 1	0.916	0.211	0.663	0.383	< 0.001	3276
Test 2	0.922	0.221	0.394	0.390	< 0.001	7221
Hatching Test 1	0.744	0.317	0.822	0.304	0.998	651
Test 2	0.650	0.455	0.653	0.442	0.573	644.5
Shadow Test 1	0.840	0.339	0.306	0.286	< 0.001	9576
Test 2	0.741	0.416	0.436	0.403	< 0.001	1247

6.2.1 Effect of distance-encoded *surface* visualization

Both tests comparing each a distance-encoded surface visualization and a Gouraud shaded visualization of a vascular model showed *highly significant benefits* from the explicit distance encoding. Subjects were also significantly faster in judging depth.

The motivation to develop this technique had been the direct projection of hepatic vascular structures onto a liver surface in an operation theater. The perception of spatial depth can be significantly improved for this application.

6.2.2 Effect of using *hatching* strokes to communicate shape

Using hatching strokes to communicate the shape of an object is a very common illustration technique and is often used in non-photorealistic rendering. However, we are not aware of any previous study comparing this technique to Gouraud or Phong shading.

Both tests comparing each a surface-hatched and a Gouraud shaded visualization revealed *no significant difference* between these techniques. Results indicate a slight advantage in using Gouraud shading but given the large number of subjects we can state that our hatching algorithm does equally well communicate the shape of objects.

6.2.3 Effect of distance-encoded *shadow*

Both tests comparing depth judgments with and without employing distance-encoded shadow revealed a *highly significant advantage* using depth-encoded shadow. Subjects also have been significantly faster in their decision using the depth cues provided by the distance-encoded shadows. The study did not reveal any significant differences between the performance of subjects, which were given an explanation about the distance-encoding in the shadows and of those who did not get these hints.

6.2.4 Subjective preference of shadow appearance

Since subjects were asked to decide on one of the two presented images, it is not strictly appropriate to analyze these results using a standard test of significance. However, it is possible to gain insight into the nature of the results by comparing each score with the theoretical result, which would have been obtained, had there been no preference for either illustration.

Subjects showed a strong preference ($p<0.001$) for providing a double-encoding of depth by adapting the length of the shadow and modulating the hatching stroke width. Asked about their preference being faced with the choice of adapting the shadow length or the shadow's hatching stroke width revealed a highly significant ($p<0.001$) preference for modulating the hatching stroke's width. Subjects also expressed their preference for hatching strokes that have a diagonal orientation to the centerline ($p<0.001$).

7 Conclusions and Future Work

New methods and algorithms for the spatial accentuated illustration of vascular structures have been described. The techniques use texture to efficiently communicate shape and topology without the requirement of a medium able to display color. Hence, color may be used to encode additional information. The techniques make substantial use of modern graphic processors, thus enabling modifications of the illustrations at interactive frame rates.

Beside introducing improved hatching, distance-encoded surface and shadow illustration, the paper's main contribution is the quantitative evaluation of these illustration techniques. The studies clearly indicate the possibilities and advantages of a direct depth encoding in 3D illustrations. For the first time, a large quantitative study substantiates the equally well communication of shape using hatching strokes compared to Gouraud shading commonly used for the same purpose.

Currently, the significant amount of polygons used to model the vascular structures is the main bottleneck in the display process. Approximating the visible geometry by planar polygon strips that always face the observer as proposed in [22] could speed up the illustration.

8 Acknowledgments

The authors wish to thank Wolfram Lamadé, MD, Robert-Bosch Hospital Stuttgart, Germany and Lüder Kahrs, Institute for Process Control and Robotics, University of Karlsruhe, Germany for the fruitful discussion and initial clinical tests. The thoughtful comments of the anonymous reviewers were also appreciated.

References

[1] K. Bühler, P. Felkel, and A. L. Cruz. Geometric methods for vessel visualization and quantification - a survey. In G. Brunnet, B. Hamann, and H. Müller, eds., *Geometric Modeling for Scientific Visualization*. Springer Verlag, 2004.

[2] E. A. Bier and K. R. Sloan. Two-part texture mapping for ray tracing. *IEEE Computer Graphics & Applications*, 6(5):40–53, Sept. 1986.

[3] J. Bloomenthal and K. Shoemake. Convolution Surfaces. In *Proc. of ACM SIGGRAPH Conference on Computer Graphics (Las Vegas, July 1991)*, pp. 251–256, 1991.

[4] T. Boskamp, H. Hahn, M. Hindennach, S. Zidowitz, S. Oeltze, B. Preim, and H.-O. Peitgen. Geometrical and structural analysis of vessel systems in 3d medical image datasets. In C. T. Leondes, ed., *Medical Imaging Systems Technology*, vol. 5, World Scientific, 2005.

[5] O. Deussen and T. Strothotte. Computer-generated pen-and-ink illustration of trees. In *Proc. of ACM SIGGRAPH Conference on Computer Graphics (New Orleans, July 2000)*, pp. 13–18, 2000.

[6] F. Dong, G. J. Clapworthy, H. Lin, and M. A. Krokos. Non-Photorealistic Rendering of Medical Volume Data. *IEEE Computer Graphics & Applications*, 23(4):44–52, July/Aug. 2003.

[7] P. Felkel, R. Wegenkittl, and K. Bühler. Surface models of tube trees. In *Computer Graphics International*, pp. 70–77, 2004.

[8] J. Ferwerda. »hi-fi« rendering. In *Proc. of ACM Siggraph/Eurographics Campfire on Perceptually Adaptive Graphics*, 2001.

[9] J. Fischer, D. Bartz, and W. Straßer. Illustrative display of hidden iso-surface structures. In *Proc. of IEEE Visualization (Minneapolis, Oct. 2005)*, pp. 663–670, 2005.

[10] B. Freudenberg. *Real-Time Stroke-Based Halftoning*. PhD thesis, Otto-von-Guericke Universität Magdeburg, 2004. Der Andere Verlag, Tönning, Lübeck und Marburg.

[11] H. K. Hahn, B. Preim, D. Selle, and H.-O. Peitgen. Visualization and interaction techniques for the exploration of vascular structures. In *Proc. of IEEE Visualization (San Diego, Oct. 2001)*, pp. 395–402, 2001.

[12] D. House, A. Bair, and C. Ware. On the optimization of visualizations of complex phenomena. In *Proc. of IEEE Visualization (Minneapolis, Oct. 2005)*, pp. 87–94, 2005.

[13] G. S. Hubona, P. N. Wheeler, G. W. Shirah, and M. Brandt. The relative contribution of stereo, lighting, and background scenes in promoting 3d depth visualization. *ACM Transactions on Computer-Human Interaction*, 6(3):214–242, Sept. 1999.

[14] V. Interrante, H. Fuchs, and S. M. Pizer. Conveying the 3d shape of smoothly curving transparent surfaces via texture. *IEEE Transactions on Visualization and Computer Graphics*, 3(2):98–117, Apr./June 1997.

[15] S. Kim, H. Hagh-Shenas, and V. Interrante. Conveying shape with texture: experimental investigations of texture's effects on shape categorization judgments. *IEEE Transactions on Visualization and Computer Graphics*, 10(4):471–483, July/Aug. 2004.

[16] Y. Masutani, K. Masamune, and T. Dohi. Region-Growing-Based Feature Extraction Algorithm for Tree-Like Objects. In *Visualization in Biomedical Computing*, vol. 1131 of *LNCS*, pp. 161–171, 1996.

[17] S. Oeltze and B. Preim. Visualization of Vascular Structures with Convolution Surfaces: Method, Validation and Evaluation. *IEEE Transactions on Medical Imaging*, 25(4):540–549, 2005.

[18] L. M. Parsons. Inability to reason about an object's orientation using an axis and angle of rotation. *Journal of Experimental Psychology: Human Perception and Performance*, 21(6):1259–1277, 1995.

[19] E. Praun, H. Hoppe, M. Webb, and A. Finkelstein. Real-time hatching. In *Proc. of ACM SIGGRAPH Conference on Computer Graphics (Los Angeles, Aug. 2001)*, pp. 579–584, 2001.

[20] V. S. Ramachandran. Perceiving shape from shading. *Scientific American*, 259(2):58–65, Aug. 1988.

[21] A. J. Stewart. Vicinity shading for enhanced perception of volumetric data. In *Proc. of IEEE Visualization (Seattle, Oct. 2003)*, pp. 355–362, 2003.

[22] C. Stoll, S. Gumhold, and H.-P. Seidel. Visualization with stylized line primitives. In *Proc. of IEEE Visualization (Minneapolis, Oct. 2005)*, pp. 695–702, 2005.

[23] B. F. Tomandl, N. C. Köstner, M. Schempershofe, W. J. Huk, C. Strauss, L. Anker, and P. Hastreiter. Ct angiography of intracranial aneurysms: A focus on postprocessing. *Radiographics*, 24(3):637–655, May/June 2004.

[24] L. R. Wanger. The effect of shadow quality on the perception of spatial relationships in computer generated imagery. In *Proc. of Symposium on Interactive 3D Graphics (Cambridge, Mar. 1992)*, pp. 39–42, 1992.

[25] L. R. Wanger, J. A. Ferwerda, and D. P. Greenberg. Perceiving spatial relationships in computer-generated images. *IEEE Computer Graphics & Applications*, 12(3):44–58, May/June 1992.

[26] C. Weigle and R. M. Taylor, II. Visualizing intersecting surfaces with nested-surface techniques. In *Proc. of IEEE Visualization (Minneapolis, Oct. 2005)*, pp. 503–510, 2005.

[27] J. Zander, T. Isenberg, S. Schlechtweg, and T. Strothotte. High quality hatching. *IEEE Computer Graphics Forum*, 23(3):421–430, 2004.

Figure 13: Hepatic venous vascular system displayed using the hatching algorithm and one distance-encoded shadow mask. The drainage areas of major vascular branches have been colored (reconstructed from MR data, 67k triangles).

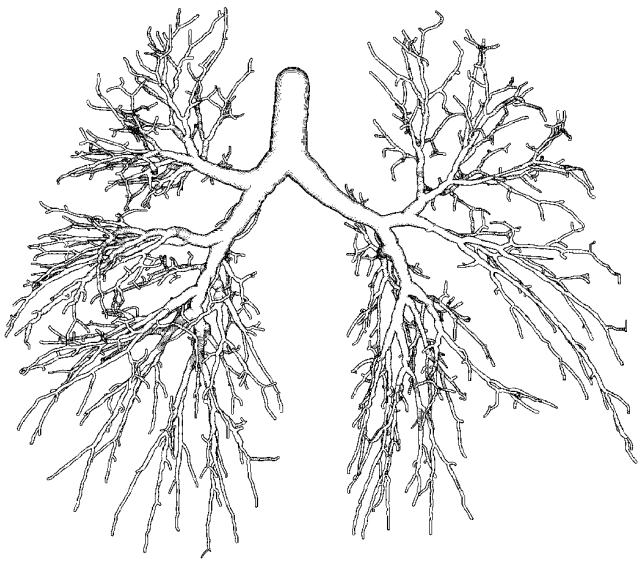

Figure 14: Bronchial tree of the lung (reconstructed corrosion cast, CT data, 230k triangles)